



The Manufacturing Engineering Society International Conference, MESIC 2015

## A Comparison between Discrete and Continuous Scanning with Conoscopic Holography

P. Zapico<sup>a</sup>, P. Fernández<sup>a</sup>, D. Blanco<sup>a</sup>, G. Valiño<sup>a</sup>, J.C. Rico<sup>a,\*</sup>

<sup>a</sup>*Dept. of Manufacturing Engineering, University of Oviedo, Campus of Gijón, 33203 Gijón*

---

### Abstract

Low density digitizing is a suitable approach for verification distances between pairs of machined flat surfaces. When defining a digitizing procedure of this type of features, two approaches could be applied: discrete or continuous scanning. Discrete Scanning (D) is performed with a static sensor, but the information for each single measurement comes from a constrained area. On the other hand, since Continuous Scanning (C) is carried out with a moving sensor, the information for each single measurement comes from a swept area. In this work, a comparison between these two approaches, when digitizing with a Conoscopic Holography sensor, is performed. The main objective is to establish their influence upon surface reconstruction quality and, thereafter, upon measurement reliability.

© 2015 The Authors. Published by Elsevier Ltd. This is an open access article under the CC BY-NC-ND license (<http://creativecommons.org/licenses/by-nc-nd/4.0/>).

Peer-review under responsibility of the Scientific Committee of MESIC 2015

*Keywords:* Conoscopic Holography; scanning; reliability.

---

### 1. Introduction

Tasks involving inspection and/or verification of manufactured parts are becoming increasingly important in modern highly-competitive markets, where product quality and cost reduction show up as key issues. Under these circumstances, non-contact measuring systems have become of great importance in the field of quality control,

---

\* Corresponding author. Tel.: +34-985-182-062 fax: +0-000-000-0000 .  
E-mail address: [jcarlosr@uniovi.es](mailto:jcarlosr@uniovi.es)

because they allow to reduce inspection times, whereas accomplishing similar accuracies to those of traditional contact systems.

Contact measurement systems are undoubtedly the most used for verification and measurement tasks. A huge research effort has been carried out on these systems, which has led to a wide knowledge on their behaviour under different conditions. Research works in this field comprehend not only the degree of influence of internal sensor structure upon instrument accuracy [1], but also the influence of parameters regarding surface characteristics (like roughness or rigidity) of the measured surface [2]. Conversely, research effort has been less intense in the field of contactless systems and, specially, in those emerging or less-spread technologies. This is the case of the Conoscopic Holography [3] technology, a type of interferometric technique with interesting capabilities, since few studies have dealt with its performance in industrial verification tasks [4, 5].

Present work will attempt to assess the capability of a conoscopic system for verifying the distance between two parallel flat surfaces. Results will be compared with those obtained by contact, which will be taken as reference. The sensor used in this work has been integrated in a Coordinate Measurement Machine (CMM), which enables both contact and contactless measurements (using Conoscopic Holography) on the same machine. Furthermore, this type of integration allows two types of measurement procedures: Discrete digitizing (D) and Continuous digitizing (C). C procedure allows for a higher digitizing speed, when compared with D. This capacity lead to collecting a higher number of surface points during equivalent periods of time, which means that a higher density of points could be obtained without increasing inspection time. It is well-known that the number of captured points and their distribution influences the measurement results, and affect calculation of parameters such as flatness or cylindricity [6-8]. In present work, density of points has also been taken into account during the evaluation of measurement system performance.

## 2. Materials and Methods

### 2.1. Equipment

A conoscopic sensor has been integrated in a DEA Swift CMM. This machine, when mounted with a touch-probe sensor, has been certified with a Maximum Permissible Linear Measuring Tolerance (MPLE) and Maximum Permissible Probing Tolerance (MPEP) as in Table 1.

Conoscopic measurements were obtained using an Optimet ConoPoint-10 sensor mounted on the CMM. Calibration procedure of the measuring system was realised using the methodology developed in previous works [9]. The sensor was equipped with a 50 mm focal length lens, which provides an 8 mm wide working range (WR). Main characteristics of this sensor can also be found on Table 1.

Table 1. Characteristics of Equipment.

CH Property	Value	CMM Property	Value ( $\mu\text{m}$ )
Measuring Frequency	50-9000 Hz	MPEP	4
Working Range (50 mm lens)	8 mm	MPEE	$4 + 0.25 \cdot L$ *
Standoff (50 mm lens)	44 mm		* Being L in mm

Two configuration parameters must be set before digitizing a particular surface:

- Power (P): sets the intensity of the laser beam.
- Frequency (F): sets the measurement rate and can be calculated as the reverse of the CCD sensor module charging period plus the time of discharge ( $5\mu\text{s}$ ).

P and F optimal values have to be established for each type of surface under given ambient conditions, in order to provide measures with the best achievable quality. Optical properties of part surface affect the quality of those measures, so signal quality indicators (signal to noise ratio –SNR– and Total) are used to determine the best sensor configuration [5].

## 2.2. Scanning system

Two alternative acquisition modes can be used for digitizing with a CH sensor:

- Time Acquisition Mode: measurement rate is set to the sensor previously-fixed frequency (F).
- Pulse Acquisition Mode: measurement rate is driven by each low-to-high edge received through an input channel. This trigger frequency has to be lower than F.

The sensor allows monitoring up to three incremental encoders, to synchronize each measurement with the actual position of the encoders. In the particular case of the system used in this research, the conoscopic sensor has been fixed to the secondary axis of the CMM, so that no vertical displacement is allowed and sensor movement is restrained to X and Y axis, and both correspondent encoder signals have been monitored.

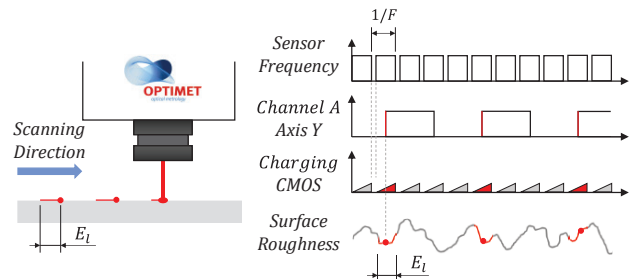


Fig. 1. Continuous scanning.

Y axis displacement signal (channel A) has been used as a trigger for the Pulse Acquisition Mode, so that movement along the Y direction is mandatory during acquisition. When a low-to-high edge triggers the sensor, the measure that is currently being integrated is assigned to the current incremental position, as registered by X and Y correspondent encoders (Fig. 1). This configuration implies that the Pulse Acquisition Mode can only provide continuous digitizing, and a constant density of points shall be obtained during Y displacements.

Whereas DEA Swift uses X4-Coded incremental encoders (with a resolution of 1 micron), the maximum achievable density for continuous digitizing along a Y trajectory is 1 point each  $4\mu\text{m}$  (one direction). This rate can be adjusted in multiples of the maximum resolution using the so-called coefficient of Dilution ( $D_c$ ). Considering this, Measuring Density ( $m_D$ ) in this research is calculated as in (1).

$$m_D = \frac{1}{4 \cdot 10^{-3} \cdot D_c} \left[ \frac{\text{measurement}}{\text{mm}} \right] \quad (1)$$

As it has been mentioned above, in the Pulse Acquisition Mode, the trigger frequency has to be lower than F. This leads to a maximum speed of movement ( $v_{\text{max}}$ ) along the Y axis, that is conditioned by F and  $D_c$  (2).

$$v_{\text{max}} = \frac{F}{m_D} \quad (2)$$

Under continuous digitizing, the sensor travels a certain distance during acquisition. This distance, known as Exposure Length ( $E_l$ ), depends on the speed of movement and can be calculated as the ratio of the speed and frequency. Since each measure in continuous digitizing is calculated considering the whole line of the surface corresponding to  $E_l$ , different values for this parameter would modify the final result, additional influence factors, like the slope of the surfaces and their roughness, are introduced.

### 3. Initial Tests

In this research, two alternative digitizing procedures have been evaluated:

- Discrete Digitizing (D): the relative position between the sensor and the scanned surface remains constant during the acquisition of each single measure. Under this procedure, triggering is driven by time. The spatial position of each single point could come from a single measure but also could be calculated as the average value of several consecutive measures upon the same location (static capture).
- Continuous Digitizing (C): the relative position between the sensor and the scanned surface varies during the acquisition of each measure, as the sensor describes a sweeping trajectory. Correspondingly, each digitized point does not represent the position of an ideal static point, but the average position of all the points swept along the exposure length (in Pulse Acquisition Mode). This approach allows for high-density digitizing of broad surfaces in short periods of time.

The first step of this research has been the evaluation of differences on sensor accuracy between D and C procedures under test conditions. An initial set of test were performed in order to analyse this question. D tests have been performed with a static positioned sensor, so 1000 consecutive measures of the same point were obtained. On the other hand, 400 consecutive scans of the same region were performed for C tests. Resultant point clouds were filtered in order to avoid the initial acceleration and final deceleration segments, and then a single centred point was selected. A Ryan-Joiner normality tests was performed upon the resultant data due to the presence of outliers. Standard deviation for both approaches can be found on Table 2.

Table 2. Results of the initial tests.

Digitizing Procedure	Standard Deviation ( $\mu\text{m}$ )	Minimum Number of Measurements *
Discrete Digitizing	0.423	119
Continuous Digitizing	0.272	50

\* 99% confidence level for mean estimation with uncertainty less than  $0.1\mu\text{m}$

Although values in Table 2 do not seem to be excessive, in fact the uncertainty of the spatial position of a particular point could reach up to  $\pm 1.2\mu\text{m}$  ( $3\sigma$ ). To reduce this uncertainty it seems necessary to average several consecutive measurements. With this purpose, the Central Limit Theorem (CLT) has been applied in order to determine the minimum number of consecutive measures that shall be averaged in each different procedure, in order to obtain a maximum  $0.1\mu\text{m}$  uncertainty, with a confidence limit of 99%, in the test conditions.

It has to be remarked that this procedure can be used in the D case, since it does not imply a significant increment in digitizing time. On the other hand, using this procedure in the C case will demand for repeating digitizing trajectories, which does not seem to be actually operative.

### 4. Experimental procedure

The experimental subject in this research was defined as the 3D distance between two parallel surfaces. This distance is analyzed in terms of accuracy: standard deviation (repeatability) and difference with reference value (trueness).

Each surface was defined for testing purposes as a square  $6.4 \times 6.4 \text{ mm}^2$  region belonging to a wire EDM machined stepped part (roughness parameters according to ISO 4287 -  $Ra$   $2.98\mu\text{m}$ ;  $Rz$   $18.31\mu\text{m}$ ). The vertical theoretical distance between these surfaces is 4 mm, while the horizontal distance is 96 mm. Test specimen was located and oriented so that the laser beam from the sensor was ideally orthogonal to both surfaces, and each surface is 2 mm away in different directions from the standoff distance. Optimal digitizing values for P and F were set to (2000, 3000Hz) in order to assure the best achievable quality for the measures [10].

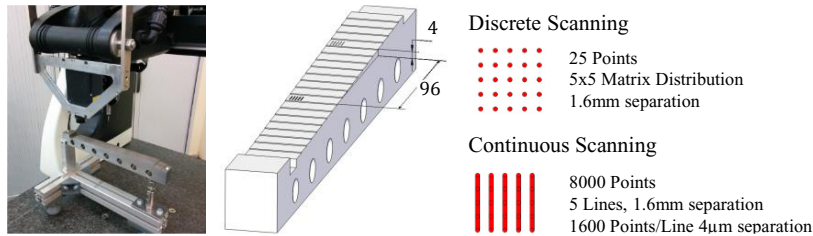


Fig. 2. Points distributions for the different procedures.

A different number of points have been established for the D and C procedures, taking into account previous considerations about correspondent scanning speeds. Therefore, the D procedure uses 25 points in a rectangular 5x5 matrix distribution, with 1.6 mm spacing between neighbour points in each direction. It has been decided that a total of 1000 consecutive measures shall be used to calculate the averaged value for the spatial position of each single point. Similarly, the C procedure uses 5 parallel trajectories along the Y axis, with a 1.6 mm spacing along the X axis. The spacing between points in the same line has been fixed to a 4  $\mu\text{m}$  value, whereas scanning speed (6 mm/s) leads to a 2  $\mu\text{m}$  value for  $E_i$ . Lines have been digitized at a constant speed, since data from both acceleration and deceleration periods have been rejected.

Two hundred experimental runs were executed during test. Each run implied the digitizing of both surfaces using both digitizing approaches (D and C). All the test period last for more than 12 hours.

Discrete and continuous procedures results have been artificially split into four methods:

- High-Density Discrete Digitizing ( $D_{HD}$ ): 25 points; each point the average of 1000 consecutive measures.
- Low-Density Discrete Digitizing ( $D_{LD}$ ): 25 points; each point a single measure.
- High-Density Continuous Digitizing ( $C_{HD}$ ): 8000 points; each point a single measure.
- Low-Density Continuous Digitizing ( $C_{LD}$ ): 25 points; each point a single measure.

The  $D_{LD}$  method was obtained from  $D_{HD}$ , identifying each point with correspondent first registered measure. Similarly,  $C_{LD}$  has been obtained from  $C_{HD}$  by selecting points corresponding with the 25 locations used in D procedures.

Once the information for each single plane and digitizing method has been obtained, corresponding point cloud is filtered to reject low-quality captures. Therefore, each plane is adjusted with the least-squares algorithm using points that simultaneously fulfil two conditions:  $\text{SNR} > 512$  and  $1200 < \text{Total} < 21000$ .

Measuring the three-dimensional measurement of distance between planes requires previous calculation of each plane centroid. Once this information has been obtained, the vector that links both centroids (vector of centroids) is also calculated. Finally, the normal vector to one plane (selected as Datum) has to be also calculated. Then, the three-dimensional distance between planes can be calculated as the scalar product of the vector of centroids by the Datum normal vector. A distance calculated using this procedure is not only sensitive to the position of both planes, but also to the orientation of the Datum plane.

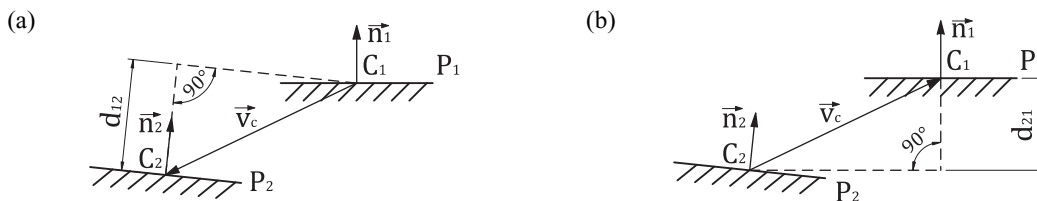


Fig. 3. 3D distance between planes.

This definition of distance between planes has been used because it is not referred to any reference system external to the scanned surfaces. It should be noted that the discrepancy between the distance measured taking one of the planes as Datum (Fig. 3.a) or the other (Fig. 3.b), will be higher the less parallel whether they are or, all the same, the more different the normal vectors are (either real differences or “artificial” ones related to calculation process). Moreover, this effect is amplified the largest is the component of the vector of centroids in the direction of higher discrepancy between normal vectors (axis of higher distance between planes).

### 5. Results

Graphic in Fig. 4 represents the evolution of distance between planes along 200 experimental runs for each of the four previously-described methods. Similarly, Table 3 provides calculated values for the averaged values and the standard deviation of this distance. The CMM Touch Probe (TP) measurement value is the reference for the distance parameter.

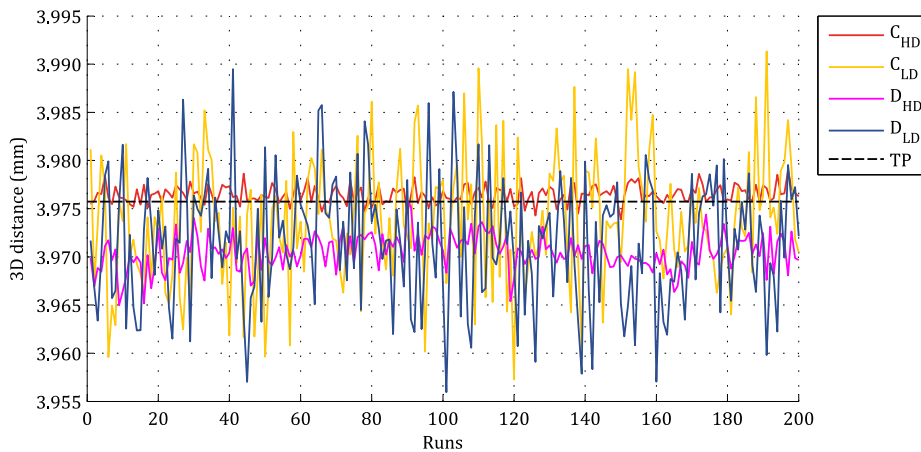


Fig. 4. 3D distances for the different methods.

The analysis of compared repeatability between those methods reveals that high-density methods provide lower standard deviations than those provided by low-density methods. It has been also found that those values clearly outmatch the results of the touch-probe scanning.

Table 3. 3D distances for the different methods.

Type	$\bar{d}_{3D}$ (mm)	$\sigma_{d_{3D}}$ ( $\mu$ m)
C <sub>HD</sub>	3.976	0.91
C <sub>LD</sub>	3.974	6.53
D <sub>HD</sub>	3.970	1.82
D <sub>LD</sub>	3.971	6.49
Touch-Probe *	3.976	5.66

\*18 runs

A deeper analysis of this behaviour links this variability to variations on the vector of centroids and/or on the Datum normal vector. Table 4 shows up the averaged values and correspondent standard deviations for the components of the vector of centroids. All these variations are relatively low (<1  $\mu$ m) with the exception of  $\sigma_{V_{ej}}$  component from C<sub>HD</sub>. This variation is related to displacements of the centroids, that are also related to the filtering of low quality points (glitter points and aberrant points).

Table 4. Centroid vector and Datum normal vector components: mean values and standard deviation.

Type	$\bar{v}_{c_i}$ (mm)	$\sigma_{v_{c_i}}$ ( $\mu\text{m}$ )	$\bar{v}_{c_j}$ (mm)	$\sigma_{v_{c_j}}$ ( $\mu\text{m}$ )	$\bar{v}_{c_k}$ (mm)	$\sigma_{v_{c_k}}$ ( $\mu\text{m}$ )	$\bar{N}_i \cdot 10^5$	$\sigma_{N_i} \cdot 10^5$	$\bar{N}_j \cdot 10^5$	$\sigma_{N_j} \cdot 10^5$	$(1 - \bar{N}_k) \cdot 10^9$	$\sigma_{N_k} \cdot 10^9$
C <sub>HD</sub>	0.065	0.458	96.019	2.073	3.980	0.55	-2.619	1.76	-3.58	0.77	1.169	0.765
C <sub>LD</sub>	0.061	0.531	96.017	0.772	3.977	0.64	-0.805	7.61	-2.46	6.72	5.503	5.640
D <sub>HD</sub>	0.059	0.112	96.017	0.295	3.977	0.48	10.317	5.92	-5.93	1.90	8.977	4.997
D <sub>LD</sub>	0.061	0.112	96.014	0.294	3.976	0.51	10.135	9.28	-4.91	6.77	12.891	10.441

In order to determine which variables are the most influent ones upon variability of 3D distance, a fit regression model has been performed, using values from the C<sub>LD</sub> runs. The components of both the vector of centroids and the Datum normal vector have been used as factors of influence. The model reveals that N<sub>j</sub> (component j from the Datum normal vector) is the most significant factor and that V<sub>c<sub>k</sub></sub> (component k from the vector of centroids) is the second one.

The great influence of N<sub>j</sub> upon 3D distance variability can be explained by the fact that distance between planes along the Y axis is much higher than those measured along other axis. It seems clear that a certain variation in the value of this component shall cause a higher variation in 3D distance than that related to a similar variation on V<sub>c<sub>k</sub></sub>. Results suggest that those methods providing a stable N<sub>j</sub> shall provide a stable 3D distance value. Values on Table 4 indicate that High-Density methods are preferable under this criterium.

Regarding trueness, Table 3 shows that there are clear differences, ranging from 0 to 6  $\mu\text{m}$ , between the averaged 3D distance, calculated with the four proposed methods, and the correspondent TP reference value. This effect is mainly caused by the differences in the Datum normal vectors (Table 4) when calculated with different methods, which are probably derived from differences between sets of points used in each case. Fig. 5.a shows an illustrative example of the differences in the adjustment of a plane caused by the election of different points from the same profile, and the effect of those differences on the orientation of normal vectors. In fact, surface characteristics of the region, like waviness and roughness, will cause those slight differences in plane adjustment when using different samples.

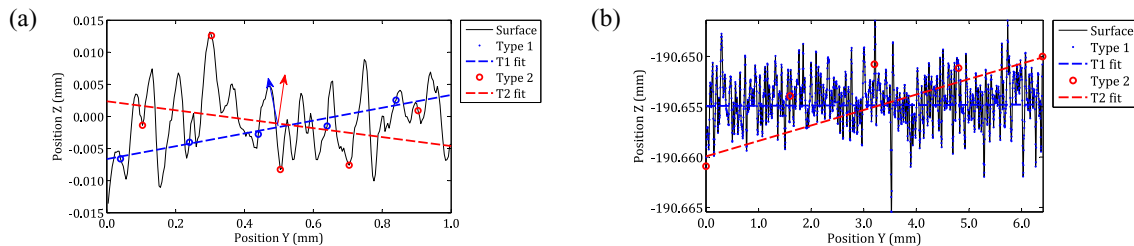


Fig. 5. Effects of different sampling points; (a) 2 types of LD sampling; (b) LD vs HD sampling.

This effect could be even more common when a comparison is established between systems with different accessibility performances. In the case analysed in this research, the spot of the conoscopic laser beam is by far smaller than the 2 mm diameter touch-probe tip. Moreover, a similar effect can also be described when comparison is held between point clouds with huge density differences. This is the case of the comparison between the high-density C<sub>HD</sub> digitizing and the other methods. Fig. 5.b. shows an example of this situation between HD adjustment and a generic LD plane.

Nevertheless, this analysis does not provide a proper explanation on the differences in trueness regarding methods D<sub>HD</sub>, D<sub>LD</sub>, C<sub>LD</sub>, since in those methods the number and theoretical location of points are all the same. Therefore, these differences should be explained introducing alternative considerations.

In this case, the relatively low difference (1 $\mu\text{m}$ ) between D<sub>LD</sub> and D<sub>HD</sub> can be explained due to intrinsically higher variability of the D<sub>LD</sub> method. On the other hand, comparatively-higher discrepancy (4 $\mu\text{m}$ ) between C<sub>LD</sub> and D<sub>HD</sub> can be related to slight differences in point information, since the dynamic nature of C<sub>LD</sub> scanning implies a larger exposition area than that of the static D<sub>HD</sub> method.



## 6. Conclusions

Performance of a CMM-integrated conoscopic sensor has been evaluated under two alternative digitizing procedures: discrete and continuous digitizing. Both approaches have been compared in the particular case of the verification of 3D distance between flat surfaces, since repeatability and trueness were calculated through long-lasting experimental runs. Additional reference values have been obtained with a touch-probe sensor and the CMM.

Regarding repeatability, it can be concluded that both procedures are equivalent under equivalent digitizing conditions (Exposition Length) for an identical number of digitized points, since standard deviation values of 3D measured distance are similar ( $C_{LD}$  and  $D_{LD}$  methods).

On the other hand, considering the assumed-as-true reference value for the 3D distance obtained with the touch-probe, significant differences had been found between different methods ( $C_{LD}$  and  $D_{LD}$ ). This result is caused by actual differences between the points used in each method, regarding either actual position of points or differences in the information in each method. No influence can be regarded to a possible lack of normality in the experimental runs, as normality it has been confirmed by a Ryan-Joiner test.

The main conclusion of this research is that the continuous digitizing high-density method ( $C_{HD}$ ) should be used when possible, since it provides higher speed and best comparative accuracy (precision plus trueness) under given test conditions. In those cases where, due to the nature or characteristics of the machine, could not be used, our recommendation is to choose the discrete digitizing high-density method ( $D_{HD}$ ).

Future works in this field will focus on analyzing the influence of variations in test conditions (such as surface orientation, roughness or exposure length) upon the recommended method.

## Acknowledgements

This work is supported by the Spanish Ministry of Economy and Competitiveness and FEDER (DPI2012-30987), the Regional Ministry of Economy and Employment of the Principality of Asturias (Spain) (SV-PA-13-ECOEMP-15) and the Government of the Principality of Asturias through the Programme “Severo Ochoa” 2014 of PhD grants for research and teaching (BP14-049).

## References

- [1] A. Weckenmann, Probing systems in dimensional metrology. *CIRP Annals-Manufacturing Technology*, 53.2 (2004), pp. 657-684.
- [2] A. Woźniak, M. Dobosz. Influence of measured objects parameters on CMM touch trigger probe accuracy of probing. *Precision Engineering*, 29.3 (2005), pp. 290-297.
- [3] G. Sirat, D. Psaltis. *Conoscopic holography*. International Society for Optics and Photonics, Los Angeles, USA (1985), pp. 324-330.
- [4] A. Paviotti, S. Carmignato, A. Voltan, N. Laurenti, G. M. Cortelazzo. Estimating angle-dependent systematic error and measurement uncertainty for a conoscopic holography measurement system. *International Society for Optics and Photonics*, 2009, 7239, pp 72390Z-1. 72390Z-12.
- [5] P. Fernández, D. Blanco, C. Rico, G. Valiño, S. Mateos. Influence of Surface Position along the Working Range of Conoscopic Holography Sensors on Dimensional Verification of AISI 316 Wire EDM Machined Surfaces. *Sensors*, 14 (2014), pp. 4495-4512.
- [6] P. B. Dhanish, J. Mathew. Effect of CMM point coordinate uncertainty on uncertainties in determination of circular features. *Measurement*, 39.6 (2006), pp. 522-531.
- [7] C. Cui, F. Shiwei, F. Huang. Research on the uncertainties from different form error evaluation methods by CMM sampling. *The International Journal of Advanced Manufacturing Technology*, 43.1-2 (2009), pp. 136-145.
- [8] A. Weckenmann, M. Knauer, H. Kunzmann. The influence of measurement strategy on the uncertainty of CMM-measurements. *CIRP Annals-Manufacturing Technology*, 47.1 (1998), pp. 451-454.
- [9] P. Fernández, D. Blanco, G. Valiño, V. Hoang, L. Suárez y S. Mateos. Integration of a conoscopic holography sensor on a CMM. *Proc. of MESIC 2011: 4th Manufacturing Society International Conference*. Cádiz, Spain, 2011.
- [10] D. Blanco, P. Fernández, P. Zapico, N. Beltrán, C. Suárez. Influence of Filtering upon Precision and Trueness in Conoscopic Holography. *Proc. of the World Congress on Engineering*. London, U.K., 2 (2014), pp. 946 – 951.